⌘ *Author's Choice*

THE JOURNAL OF BIOLOGICAL CHEMISTRY VOL. 287, NO. 28, pp. 23283–23293, July 6, 2012

Structural Characterization of Binding Mode of Smoking Cessation Drugs to Nicotinic Acetylcholine Receptors through Study of Ligand Complexes with Acetylcholine-binding Protein*[S]

Received for publication, March 8, 2012, and in revised form, April 20, 2012 Published, JBC Papers in Press, May 2, 2012, DOI 10.1074/jbc.M112.360347

Prakash Rucktooa[‡1], **Claire A. Haseler**[§], **René van Elk**[¶], **August B. Smit**[¶], **Timothy Gallagher**[§], **and Titia K. Sixma**[‡2]

From the [‡]*Division of Biochemistry and Center for Biomedical Genetics, Netherlands Cancer Institute, 1066 CX Amsterdam, The Netherlands,* [§]*School of Chemistry, University of Bristol, BS8 1TS Bristol, United Kingdom, and the* [¶]*Department of Molecular and Cellular Neurobiology, Center for Neurogenomics and Cognitive Research, VU University Amsterdam, 1081 HV Amsterdam, The Netherlands*

Background: Cytisine and varenicline are smoking cessation drugs binding to nicotinic receptors (nAChRs).
Results: We studied crystal structures of cytisine and varenicline with AChBP and analyzed binding of $\alpha4\beta2$-like or $\alpha7$-like AChBP mutants to cytisine.
Conclusion: Ligand selectivity relies on residues beyond the binding site primary shell.
Significance: These structures will contribute to designing novel compounds targeting specific nAChR subtypes.

Smoking cessation is an important aim in public health worldwide as tobacco smoking causes many preventable deaths. Addiction to tobacco smoking results from the binding of nicotine to nicotinic acetylcholine receptors (nAChRs) in the brain, in particular the $\alpha4\beta2$ receptor. One way to aid smoking cessation is by the use of nicotine replacement therapies or partial nAChR agonists like cytisine or varenicline. Here we present the co-crystal structures of cytisine and varenicline in complex with *Aplysia californica* acetylcholine-binding protein and use these as models to investigate binding of these ligands binding to nAChRs. This analysis of the binding properties of these two partial agonists provides insight into differences with nicotine binding to nAChRs. A mutational analysis reveals that the residues conveying subtype selectivity in nAChRs reside on the binding site complementary face and include features extending beyond the first shell of contacting residues.

Nicotinic acetylcholine receptors (nAChRs)[3] are cation-selective ligand-gated ion channels. They are prototypical members of the Cys-loop receptor family and are activated by neurotransmitters such as acetylcholine or choline. They also respond to numerous non-endogenous neuroactive molecules of which nicotine is the most well known (1). nAChRs are assembled as homo- or heteropentamers (2–4). The neuronal nAChR family comprises nine different α subunits and three different β subunits that contribute to a large array of receptor subtypes, posing specificity issues when addressing ligands to a specific receptor subtype. Combinations of different protomers in specific stoichiometries give rise to different nAChR subtypes, each displaying a characteristic pharmacological and biophysical profile.

Structural studies on the full-length Torpedo muscle type nAChR by cryo-electron microscopy provided a structure at 4 Å resolution (5, 6). Structural data at high resolution are available for acetylcholine-binding protein (AChBP), a water-soluble homolog of the nAChR ligand binding domain (7, 8), with various ligands (for an overview, see Ref. 1). The monomeric mouse muscle type $\alpha1$ nAChR ligand binding domain structure (9) has revealed that despite low sequence identity, AChBP protomers provide a very useful model, as they are structurally highly similar to mammalian nicotinic receptors. Recent three-dimensional structures of two different full-length prokaryotic ligand-gated ion channels (10–12) as well as that of GluCl, an invertebrate ligand-gated ion channel (13), also show high structural similarity to AChBPs. Because it is easily crystallizable, AChBP still represents the best template for the characterization of ligand binding to nAChR ligand binding domains.

Ligand binding in AChBPs and in nAChRs occurs at the interface between two adjacent protomers, with one of the subunits contributing to the principal face and the second subunit contributing to the complementary face of the ligand binding site (7, 14). In nAChRs, the principal face always arises from the α subunit, whereas the complementary face is contributed by either α- or non-α-subunits. Principal face residues are highly conserved among nAChRs and AChBPs, whereas the complementary face displays higher variability. Previous studies have shown that the complementary face residues are important in the modulation of ligand binding affinities (15, 16). Binding

* This work was supported by the European Union Seventh Framework Programme under Grant agreement HEALTH-F2–2007-202088 ("Neuro-Cypres" project) and from TiPharma Grant D2-103 (to A. B. S.).
⌘ *Author's Choice*—Final version full access.
[S] This article contains supplemental Figs. S1–S4.
The atomic coordinates and structure factors (codes 4AFO and 4AFT) have been deposited in the Protein Data Bank, Research Collaboratory for Structural Bioinformatics, Rutgers University, New Brunswick, NJ (http://www.rcsb.org/).
[1] Supported by a long term fellowship from the European Molecular Biology Organization.
[2] To whom correspondence should be addressed. E-mail: t.sixma@nki.nl.
[3] The abbreviations used are: nAChR, nicotinic acetylcholine receptor; AChBP, acetylcholine-binding protein; AcAChBP, *A. californica* AChBP; LsAChBP, *Lymnaea stagnalis* AChBP; BtAChBP, *B. truncatus* AChBP; ITC, isothermal titration calorimetry; 5HT3AR, 5-hydroxytryptamine 3 receptor.

specificity to different nAChR subtypes is known to arise at least in part from subpockets located at the apical or basal regions of the binding site (17, 18). Such subpockets are accessible to relatively large ligands, but not necessarily to smaller nicotinic ligands, likely to display affinity differences when binding to nAChRs.

Nicotine is a plant alkaloid responsible for the addictive properties of tobacco. Among others, nicotine binding to brain nAChRs results in dopamine release, which is critically involved in reward mechanisms and in the reinforcing effect of the drug (19). Different mechanisms underlying nicotine addiction are complex and have been extensively reviewed (*e.g.* Ref. 20). Nicotine replacement therapies constitute a clean and safer mode of delivery of this compound compared with smoking tobacco. Nicotine binds with high affinity to the $\alpha4\beta2$ nAChRs (K_i 1 nM), where it acts as a full agonist, as opposed to low affinity binding to the $\alpha7$ receptor (K_i 1600 nM) (21). Nicotine application provides a high level of occupancy at $\alpha4\beta2$ nAChRs, maintaining them in a desensitized state associated with a reduced nicotinic functional activity (19). A novel treatment option in smoking cessation is the use of nAChR partial agonists. Partial agonists may have a therapeutic effect due to two critical molecular actions, which are to desensitize $\alpha4\beta2$ nAChRs and to induce channel opening with higher affinity but with lower efficacy than a full agonist at equal receptor occupancy. This diminishes nicotine reinforcement and reduces the pleasure from smoking, thus aiding the continued adherence to therapy (19).

One of the $\alpha4\beta2$ nAChR partial agonists used for smoking cessation is cytisine, a toxic plant alkaloid isolated from *Cytisus laburnum* (22). This natural product has been used as a lead compound in the development of varenicline (23), commercialized as Champix® or Chantix® by Pfizer. Varenicline also functions as a partial agonist at the $\alpha4\beta2$ nAChRs, and both cytisine and varenicline display high affinities, with K_i values of 0.17 and 0.06 nM, respectively, for this receptor subtype, whereas they bind with lower affinity to the $\alpha7$ nAChR, with K_i values of 4200 and 322 nM, respectively (21, 23). In smoking cessation therapies, application of these molecules provides a 1.5–3-fold increase in chances for quitting smoking compared with the use of placebos (19).

To understand the basis for subtype-selective and high affinity binding of partial agonists to nAChRs, we have structurally characterized complexes of *Aplysia californica* AChBP (AcAChBP) with the small $\alpha4\beta2$ partial agonists cytisine and varenicline and compare these to an LsAChBP complex with the $\alpha4\beta2$ agonist nicotine. We have complemented these structural studies with ligand binding studies to determine affinities. and we discuss the thermodynamic profiles of these compounds when binding to AcAChBP. These three ligands display differences in affinity when binding to different nAChR subtypes. They indeed bind to $\alpha4\beta2$ receptors with higher affinity compared with the $\alpha7$ subtype. We, therefore, assessed cytisine binding to wild type and mutant AcAChBPs engineered to reflect either $\alpha7$ or $\alpha4\beta2$ ligand binding sites to learn about selectivity properties for these receptors. Our data may contribute to further design efforts aiming at the generation of optimized subtype-specific (partial) agonists targeting nAChRs.

EXPERIMENTAL PROCEDURES

Protein Expression and Purification—AcAChBP used in crystallization or in ITC assays was expressed as untagged protein in Sf21 insect cells using the baculovirus expression system and purified from growth medium as described previously (24). AcAChBP mutants were expressed in HEK293 cells for radioligand binding assays. A synthetic gene, codon optimized for expression in mammalian cells, coding for AcAChBP downstream of a preprotrypsin signal peptide, was purchased (Genscript) and was cloned into a pTT3 vector using BamHI and HindIII as restriction sites. The resulting plasmid was transfected into attached HEK293 cells, and medium harvested 4 days after transfection was processed as above for purifying wild type and mutant AcAChBP variants.

Crystallization—Untagged AcAChBP concentrated to 3 mg/ml was incubated on ice for 1 h with 1 mM ligand before vapor diffusion crystallization trials were set up. Co-crystals for the different ligands grew in similar conditions at room temperature in 0.6–1.2 M ammonium sulfate, 0.1 M MMT buffer at a pH ranging between 6.5 and 8.5. Crystals were cryoprotected in mother liquor supplemented with 25% glycerol and 1 mM ligand before they were flash-frozen in liquid nitrogen.

Structure Solution and Refinement—Data were collected on beamlines ID14-4 or on beamline PX1 at SLS (Switzerland) (Table 1). Cytisine and varenicline co-crystals were in space-group I23 and diffracted to resolutions of 2.9 and 3.2 Å, respectively (Table 1). Data reduction was done either using XDS and XSCALE (24–26) or using MOSFLM and SCALA (27). Molecular replacement trials were performed using PHASER (28) with PDB code 2BR7 (29) as the search model. The cytisine and varenicline co-crystals contained one pentamer in the asymmetric unit. Iterative structure refinement was performed using either REFMAC (30) from the CCP4 suite or BUSTER (31). Non-crystallographic symmetry (NCS) restraints were maintained throughout the refinement procedure using local NCSR as implemented in REFMAC or in a local version of the PDB_REDO script (32) or using the local similarity structure restraint from BUSTER. Thanks to this use of 5-fold symmetry restraints, electron density maps are much better than usual at these resolutions. One TLS group per chain was used in refinement, and both the x-ray weight and B-factor restraint weight were optimized to reduce the R_{work}/R_{free} gap during refinement. Refinement was interspersed with manual rebuilding in COOT (33). All protomer-protomer interfaces enclosed a ligand molecule that was built into the electron density only in later refinement stages. All ligand molecules were well defined in electron density. Refined structures were validated using the Molprobity server (34). The figures were generated using PyMOL. Structures have been deposited in the PDB with accession codes 4AFO (cytisine) and 4AFT (varenicline), respectively.

Binding Assays—Isothermal titration calorimetry experiments were performed on either a VP-ITC microcalorimeter (Microcal) or on an iTC200 system (Microcal) at 25 °C. AcAChBP used in these experiments was dialyzed in a buffer containing 20 mM TRIS-Cl, pH 8, and 150 mM NaCl. The ligands investigated were dissolved in the same buffer. For a

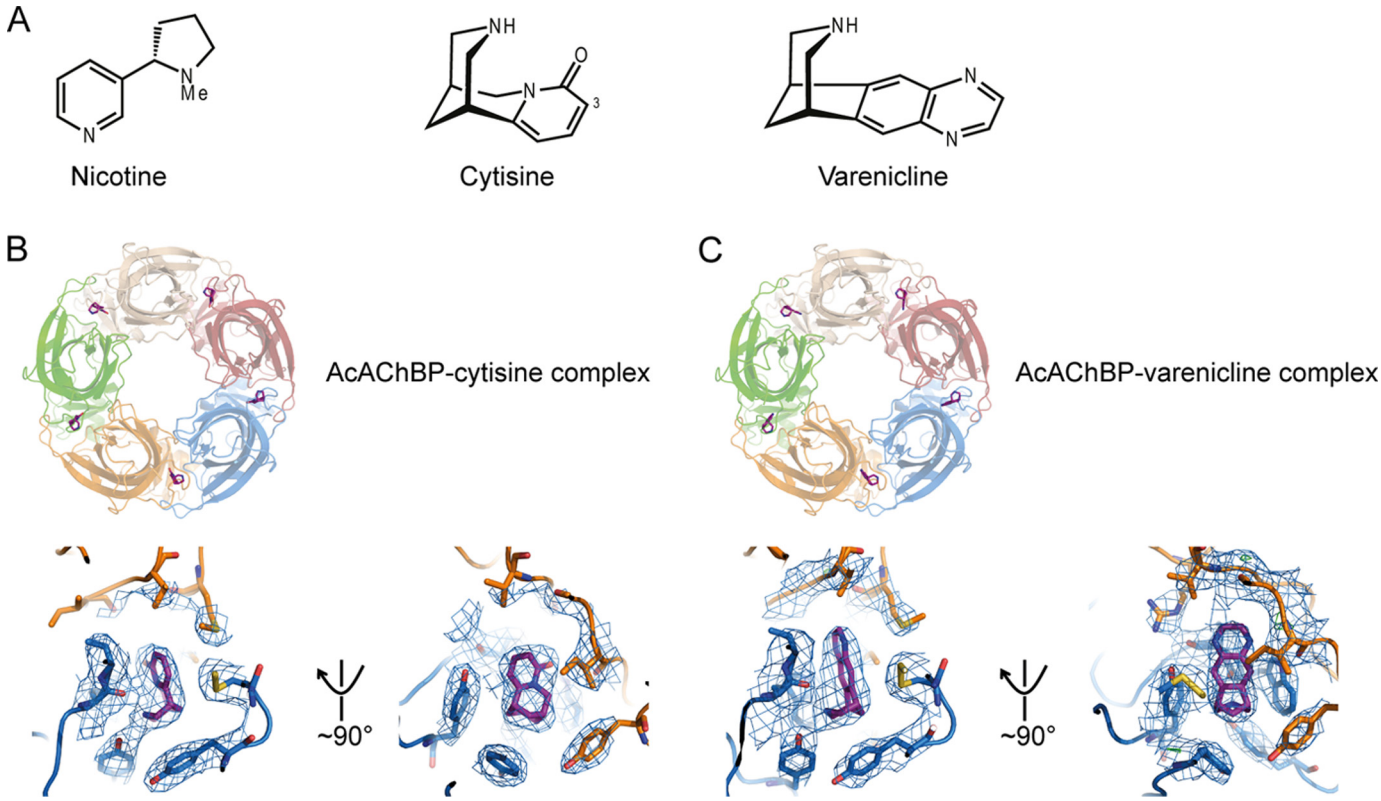

FIGURE 1. *A*, shown are chemical structures of ligands used in this work: nicotine, cytisine, and varenicline. Bottom views of AcAChBP in complex with cytisine (*B*) and varenicline (*C*) are shown. Each chain of the pentameric assembly is colored differently. Two blown-up views of one protomer-protomer interface are provided for cytisine (*left*) and for varenicline (*right*), with interacting residues represented using *sticks* and placed in the δA-weighted $2mF_o - dF_c$ electron density map contoured at 1σ (*blue mesh*), carved 6.5Å around the ligands. In these blown-up views, principal face residues are in *blue*, whereas the complementary face residues are colored *orange*.

typical experiment, 100 μM concentrations of ligand were titrated into 10 μM AcAChBP. Titration of ligands into buffer alone was performed to determine the change in enthalpy generated by the dilution of the ligands, and this background was subtracted from the actual ligand binding experiments. Corrected data were analyzed using manufacturer supplied software and were fitted using a non-linear least squares method with a single-site binding model.

Radioligand binding assays through either classical saturation experiments or through homologous competition were performed with AcAChBP in buffer (20 mM Tris, pH 7.4, 0.05% Tween) in a final assay volume of 100 μl in Optiplates (PerkinElmer Life Sciences). [^{3}H]Cytisine concentration (PerkinElmer; specific activity, ~40 Ci/mmol) was around the K_d value for the target protein. The amount of protein (4–300 ng) was chosen such that a clear window in the homologous saturation curve was obtained with sufficient events in scintillation counting and a radioligand depletion of less than 10%. WGA-YSI SPA beads (PerkinElmer) were added at 2 mg/ml final concentration. Plates were incubated at room temperature under continuous shaking and protected from light for 1.5 h. SPA beads were allowed to settle for 3 h in the absence of light before counting. The label-bead complex was counted in a Wallac 1450 MicroBeta (PerkinElmer). All radioligand binding data were fitted to a one site homologous competitive binding model using Graphpad Prism® (Version 5, GraphPad Software, Inc., San Diego, CA). At least three independent repeats were performed for the experiments.

TABLE 1

Crystallographic parameters for the AcAChBP co-crystal structures with cytisine and varenicline

	AcAChBP-Cytisine	AcAChBP-Varenicline
Data collection	ESRF ID14-4	SLS PX1
Space group	*I23*	*I23*
Cell dimensions		
a, *b*, *c* (Å)	206.69	207.3
α, β, γ (°)	90, 90, 90	90, 90, 90
Resolution (Å)	48.72-2.88 (3.04-2.88)	48.86-3.20 (3.37-3.20)
R_{merge} (%)	14.3 (85.9)	9.7 (90.5)
R_{pim} (%)	7.0 (42.6)	7.1 (68.3)
$I/\sigma I$	10.0 (1.7)	7.8 (1.1)
Completeness (%)	95.7 (88.7)	94.3 (97.3)
Redundancy	5.0 (4.9)	2.4 (2.4)
Refinement		
Resolution (Å)	48.72-2.88	73.4-3.2
No. reflections	31,313	21,800
R_{work}/R_{free}	18.5/22.4	18.8/20.8
No. atoms		
Protein	8,213	8,213
Ligand/ion	82	80
Water	24	0
B-factors (Å^2)		
Protein	50.4	101.2
Ligand/ion	45.7	92.0
Water	29.3	–
Root mean square deviations		
Bond lengths (Å)	0.011	0.005
Bond angles (°)	1.51	1.06
Poor rotamers (%)	2.23	0.85
Ramachandran outliers (%)	0	0
Ramachandran favored (%)	99.21	98.33
Clash score (percentile)	98th	95th
Overall score (percentile)	100th	100th

RESULTS AND DISCUSSION

We have validated the binding of three different high affinity α4β2 ligands (Fig. 1*A*) currently used as smoking cessation aids,

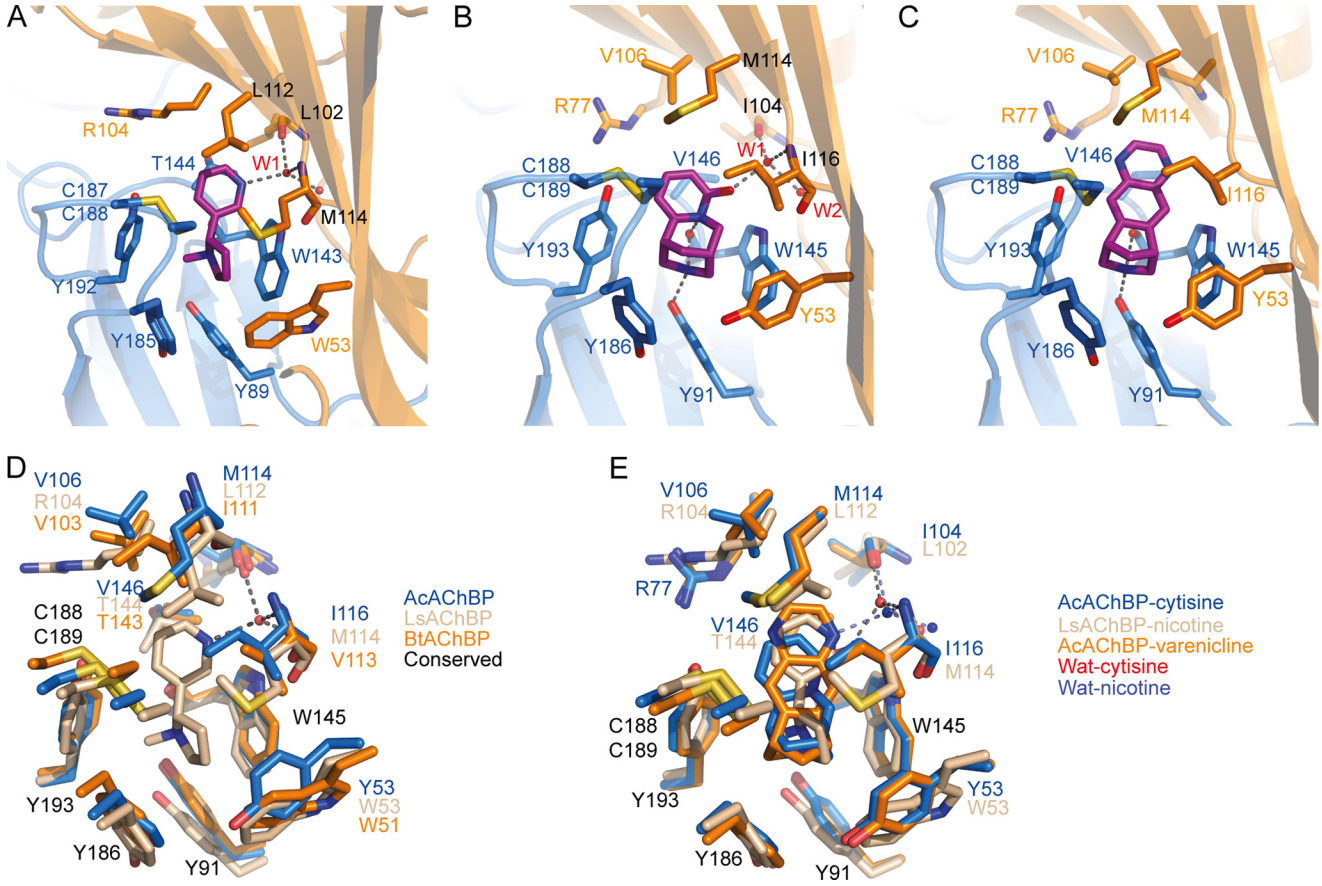

FIGURE 2. Detailed views of the Ls- (*A*) or AcAChBP (*B* and *C*) binding sites are depicted. Principal face residues are colored *blue*, whereas complementary face residues are colored *orange*. Interacting residues are represented as *sticks*, and water molecules are shown as *spheres*. The nicotine-LsAChBP complex (PDB code 1UW6) (*A*), cytisine-AcAChBP complex (*B*), and varenicline-AcAChBP complex (*C*) are represented. *D*, shown is secondary structure matching superposition (53) of binding site principal faces of Ac-, Ls- (PDB code 1UW6), and BtAChBPs (PDB code 2BJ0, ligand omitted for clarity). Interesting, residues are represented as *blue*, *silicon*, and *orange sticks*, respectively, to outline the variability among the binding sites. For conserved residues, AcAChBP numbering is provided. *E*, shown is secondary structure matching superposition (53) of binding site principal faces of AcAChBP in complex with cytisine (*blue*) and varenicline (*orange*) and of LsAChBP in complex with nicotine (PDB code 1UW6). Interacting residues are represented as *sticks* to allow a comparison of binding modes for these ligands. For conserved residues, AcAChBP numbering is provided.

namely (−)-nicotine, (−)-cytisine, and (*meso*)-varenicline to AcAChBP. We then proceeded with the structural characterization of complexes of AcAChBP with cytisine and varenicline refined to resolutions of 2.9 and 3.2 Å, respectively (Table 1). Cytisine and varenicline co-crystals grew in similar conditions in space group I23 with one pentamer in the asymmetric unit (see "Experimental Procedures") and display similar homopentameric organization as previously solved AChBP structures (for review, see Ref. 1). The electron density maps for these structures were much better than expected for such resolutions thanks to the use of 5-fold non-crystallographic symmetry restraints during refinement, and we could confidently build the ligands in the binding sites (Fig. 1, *B* and *C*, and supplemental Fig. S1). All protomer-protomer interfaces in these complexes encompassed their respective ligands (Fig. 1, *B* and *C*) with the C loop closed over the ligand binding site. Tips of the C-loops from different protomers were not involved in crystal packing. All the ligands above are enclosed in the characteristic aromatic cage constituted of residues Tyr-91, Trp-145, Tyr-186, and Tyr-193 from the principal face and residue Tyr-53 from the complementary face. Hydrophobic interactions from disulfide-bonded Cys-188 and Cys-189 from loop C further stabilized the ligands in the binding site. We further compared binding modes of $\alpha4\beta2$ partial agonists cytisine and varenicline with that of nicotine in complex with LsAChBP (14).

Cytisine Complex—Cytisine is a plant alkaloid that acts as a partial agonist at the $\alpha4\beta2$ subtype nAChRs, with an EC_{50} of ~1 μM (22, 35). Our co-crystal structure of AcAChBP with cytisine was solved with a resolution of 2.9 Å and contains one AcAChBP pentamer per asymmetric unit. All five binding sites in the pentamer are occupied by cytisine, and the ligand adopts the same orientation in all sites (Fig. 2*B*).

The piperidine ring of cytisine is oriented toward the basal side of the ligand binding site, whereas the pyridone ring is oriented toward the apical side. On top of the hydrophobic interactions involving the binding site aromatic cage residues (Tyr-91, Trp-145, Tyr-186, and Tyr-193), the tip of loop C (Cys-188 and Cys-189), and complementary face residues Met-114 and Ile-116, cytisine is stabilized through hydrogen bonds between the carbonyl group of Trp-145 and the pyridone ring N2 as well as between the piperidine ring N1 and the hydroxyl moiety of Tyr-91 or the Trp-145 backbone carbonyl. The cytisine oxygen is also hydrogen-bonded to a water molecule (W1) stabilized by the carbonyl backbone of Ile-104, the Ile-116 backbone amide from the complementary face, and a second water

molecule (W2). This binding mode involving water molecules is highly reminiscent of nicotine binding in LsAChBP (Fig. 2*A*) (14). Further hydrophobic interactions from the side chains of Val-146 from the principal face and Met-114 and Ile-116 from the complementary face also stabilize the ligand.

Ring-substituted cytisine derivatives have been generated previously to further investigate affinity and/or selectivity variations in binding to the $\alpha4\beta2$ receptor subtype (36, 37). These cytisine derivatives mainly target the pyridone ring (21, 38, 39) or the piperidine ring nitrogen (21, 38, 40). Methylation of the piperidine ring nitrogen, yielding caulophylline, induces a significant loss in affinity toward the $\alpha4\beta2$ nAChRs, likely due to steric hindrance with Tyr-91. However, interestingly a larger substitution involving a 3-ketobutyl moiety drastically increases the affinity of the cytisine derivative for the $\alpha4\beta2$ subtype receptors, toward which it also acts as an antagonist (40). Systematic *N*-substitutions performed on the cytisine piperidine ring show that variations in affinities of cytisine derivatives result from the size of the substituent and its electron withdrawing nature (41). We have shown recently that Tyr-91 in the AcAChBP binding site can re-orient its side chain to accommodate larger ligands (24). Such a rearrangement could explain an improved binding affinity of a larger ligand for the $\alpha4\beta2$ receptors. The Tyr-91 equivalent in the $\alpha4\beta2$ nAChRs could indeed potentially be stabilized through hydrogen bonds to the $\beta2$ loop F Asp-168. However, given the high degree of sequence variability observed in this region in nAChRs, such stabilization of the Tyr-91 equivalent in $\alpha4\beta2$ is hard to predict. Halogenated cytisine derivatives such as the 3-chloro- or 3-bromocytisine display higher affinity toward the $\alpha4\beta2$ nAChRs compared with cytisine (21, 38, 39). Our AcAChBP-cytisine complex structure suggests that the presence of a chloro or bromo moiety at C(3) would increase hydrophobic interactions with the surrounding binding site residues.

Cytisine docking studies into LsAChBP (42) or into $\alpha4\beta2$ receptors and have been performed (41). The docking trials in LsAChBP predicted an orientation that agrees well with the AcAChBP co-crystal structure (42). In contrast, the predictions based on docking of unmodified cytisine into either rat- or human $\alpha4\beta2$-modeled nAChR binding sites indicates that the two different minimum energy poses of cytisine differ between these two species, each of which is different from our AcAChBP-cytisine co-crystal structure, with the ligand pyridone ring oriented toward the basal region of the binding sites (41). The lack of robustness of this prediction and the disparity from the nicotine binding suggests that these docking studies are likely to be incorrect.

Varenicline Complex—Varenicline was developed by Pfizer as medication to assist in smoking cessation using cytisine as an initial lead compound. Varenicline shows an increased affinity toward $\alpha4\beta2$ nAChRs compared with its parent molecule and maintains a partial agonist activity (23). Our AcAChBP-varenicline complex structure refined to 3.2 Å indicates that the ligand is similarly oriented in all five protomer-protomer interfaces. The aromatic moiety of the ligand is oriented toward the apical region of the AChBP binding site, whereas the aliphatic moiety is oriented toward the basal region (Fig. 2*C*). The varenicline pyrazine unit extends further toward the apical region of the AcAChBP binding site than the cytisine pyridone ring. The piperidine nitrogen occupies essentially the same position as is observed for cytisine, hence making hydrogen bonds with the phenolic hydroxyl group of Tyr-91 as well as with the Trp-145 backbone carbonyl (Fig. 2*C*). Varenicline is very rigid with a planar quinoxaline moiety and does not possess any bulky decoration. The ligand is stabilized in the AcAChBP binding site through hydrophobic interactions with the aromatic cage residues as well as the vicinal disulfide-bonded Cys-188 and Cys-189. Further hydrophobic interactions arise from the side chains of Val-146 from the principal face and from the side chains of Val-106, Met-114, and Ile-116 from the complementary face. The N3 nitrogen from the pyrazine ring superposes relatively well with the nicotine pyridine nitrogen in the LsAChBP-nicotine structure (Fig. 2*A*). This nitrogen in the LsAChBP-nicotine complex is involved in water-mediated interactions to the backbone carbonyls of residues Leu-102 and Met-114. Such a hydrogen bonding pattern is, however, not observed in our AcAChBP-varenicline structure probably because of low resolution. Docking trials of varenicline performed into homology-modeled $\alpha4\beta2$ nAChR (43) orient the ligand in a similar way to what we observe in our AcAChBP-varenicline co-crystal and preserve the hydrogen-bonding pattern of the piperidine nitrogen with the $\alpha4\beta2$ Tyr-91 and Trp-147.

Characterizing Ligand Binding to AChBP—We investigated the binding characteristics of nicotine, cytisine, and varenicline to AcAChBP using isothermal titration calorimetry (ITC), and we show that these three ligands bind with moderate affinities of 0.8, 1.6, and 0.3 μM, respectively (Fig. 3, *A–C*, Table 2).

Considering the very low binding affinity of nicotine for AcAChBP (835 nM) relative to Ls- (45 nM) or *Bulinus truncatus* (8 nM) AChBPs (14, 15), we also compared the thermodynamic profiles for nicotine binding to these different AChBPs (Fig. 3*D*). Our ITC binding experiments show that differences in affinity originate mainly from differences in the enthalpic contribution rather than the entropic contribution to the binding. Notable differences arise from variability in the complementary face residues with LsAChBP residues switched from Leu-112, Met-114, and Trp-53 to Met-114, Ile-116, and Tyr-53, respectively, in AcAChBP (Fig. 2, *D* and *E*). Whereas the Leu-112 and Met-114 substitutions to a methionine and an isoleucine, respectively, are conservative, the substitution of Trp-53, conserved in nAChRs, to Tyr-53 has been reported to account for a 90-fold difference in affinity of epibatidine for AcAChBP compared with LsAChBP (17). It is very likely that the drop in affinity observed in the binding of AcAChBP to nicotine stems mainly from the presence of a tyrosine rather than a tryptophan at position 53. We have previously shown that the affinity of AcAChBP for nicotine can be modulated through the Y53W mutation, increasing the observed affinity to that observed for LsAChBP (24).

Comparing the binding of nicotine, cytisine, and varenicline to AcAChBP (Fig. 3*E*) shows an increase in both favorable enthalpic contribution and unfavorable entropic contribution to the binding, with an increase in the size of the ligand bound at the protomer-protomer interface. Nicotine or cytisine interaction with Ls- and AcAChBP, respectively, results in a roughly

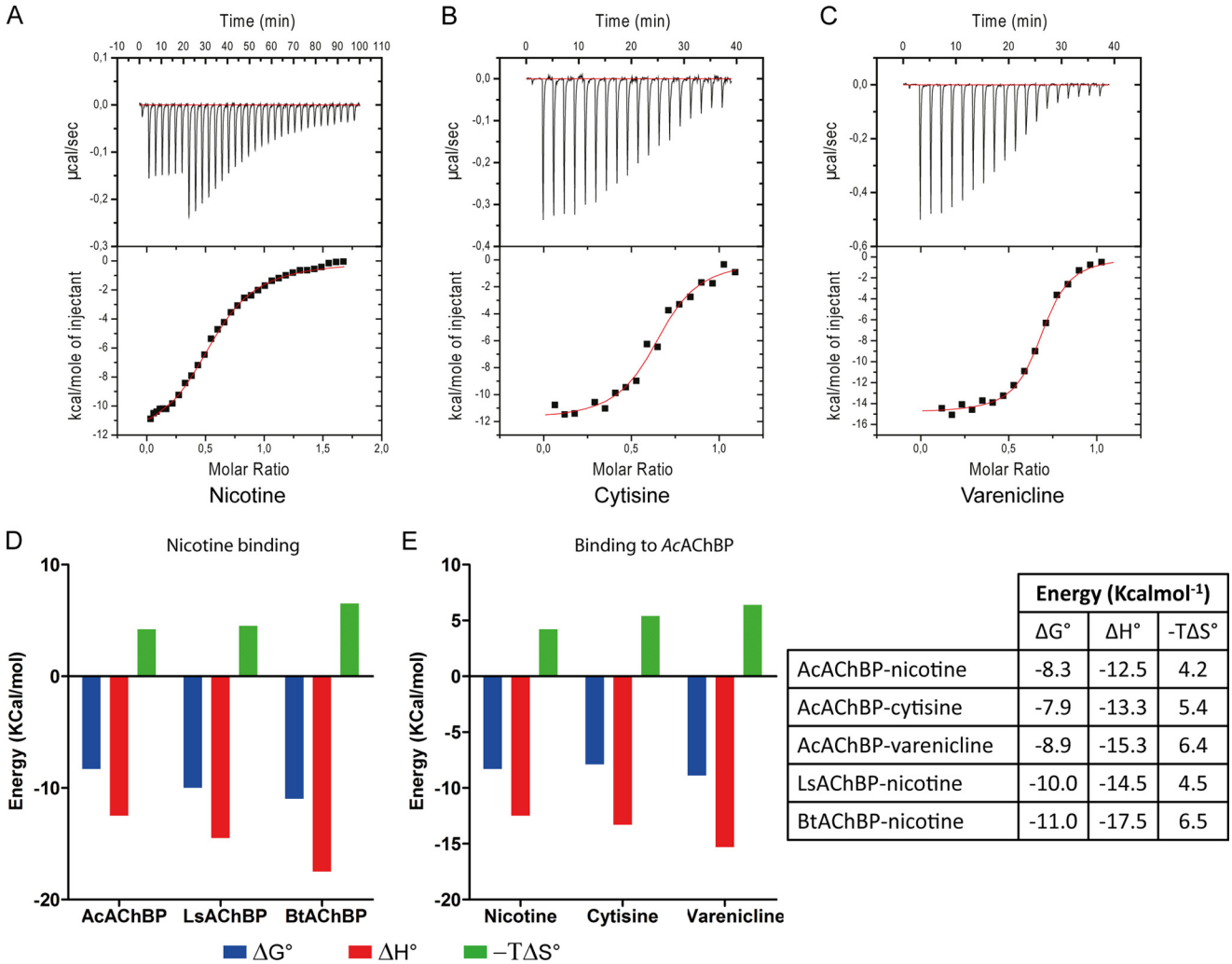

	Energy (Kcalmol^{-1})		
	ΔG°	ΔH°	-TΔS°
AcAChBP-nicotine	-8.3	-12.5	4.2
AcAChBP-cytisine	-7.9	-13.3	5.4
AcAChBP-varenicline	-8.9	-15.3	6.4
LsAChBP-nicotine	-10.0	-14.5	4.5
BtAChBP-nicotine	-11.0	-17.5	6.5

FIGURE 3. ITC titration curves for the binding of nicotine (*A*), cytisine (*B*), and varenicline (*C*) to AcAChBP are provided. Nicotine binding data were recorded on a VP-ITC instrument, whereas cytisine and varenicline binding data were recorded on an ITC200 instrument. The thermodynamic profiles for nicotine, cytisine, and varenicline binding to AcAChBP (*D*) are displayed as a *bar chart* with Gibb's energy (Δ*G*°) in *blue* and the enthalpic (Δ*H*°) and entropic contributions (−TΔ*S*°) in *red* and in *green*, respectively. A similar bar chart representation is provided for the comparison of nicotine binding to Ac-, Ls-, and BtAChBPs (*E*).

TABLE 2

Binding data of cytisine, varenicline, and nicotine are reported for α4β2 and α7 nAChRs and AcAChBP as well as nicotine binding data for LsAChBP (ITC data) and BtAChBP (ITC data)

ND, not determined.

Protein	Nicotine	Cytisine	Varenicline
α4β2 nAChR (K_i) (nM)	0.95[a]	0.17[a]	0.06[a]
α7 nAChR (K_i) (nM)	6290[a]	4200[a]	322[a]
AcAChBP (K_D) (nM)	835[b]	1640[b]	342[b]
LsAChBP (K_D) (nM)	45[c]	ND	ND
BtAChBP (K_D) (nM)	8[d]	ND	ND

[a] From Refs. 21 and 23.
[b] ITC data, this study.
[c] From Ref. 14.
[d] From Ref. 15.

similar buried surface area of 290 Å^2 according to analysis using the PISA web server (44), whereas binding of varenicline to AcAChBP results in a buried surface area of 300 Å^2. Varenicline is indeed involved in hydrophobic contacts with residues that are located further at the apical side of the binding site such as Val-106 (3.6 Å), compared with cytisine (4.6 Å). On the other hand, contrary to cytisine or varenicline, nicotine does not make any hydrogen bond with Tyr-91. This probably entails a lower enthalpic contribution in the binding of nicotine but could also result in more freedom of motion for the Tyr-91 side chain, possibly lowering unfavorable entropic contribution. However, in the case of cytisine or of varenicline, the hydrogen bond between the ligand and Tyr-91 locks this residue in one conformation and potentially increases unfavorable entropic contribution to the binding of these ligands to AcAChBP.

Binding affinity can be improved by increasing favorable enthalpic and entropic contributions, for example through the growth of the ligand. In the case of varenicline, further growth toward the apical region of the binding site is likely to result in clashes with binding site residues, such as Val-106. Further growing of this molecule could, however, be achieved by extending from the varenicline piperidine moiety to explore the basal region of the binding site. Indeed, previous data show that in AcAChBP, the Tyr-91 side chain can be reoriented to accommodate large ligands by making hydrogen bonds to Tyr-53 and to Ser-165 (17, 24) with limited entropic penalty but with an important increase in favorable enthalpic contribution (24). Such a reorientation of the Tyr-91 side chain in nAChRs is, however, hard to predict considering that Tyr-53 is substituted

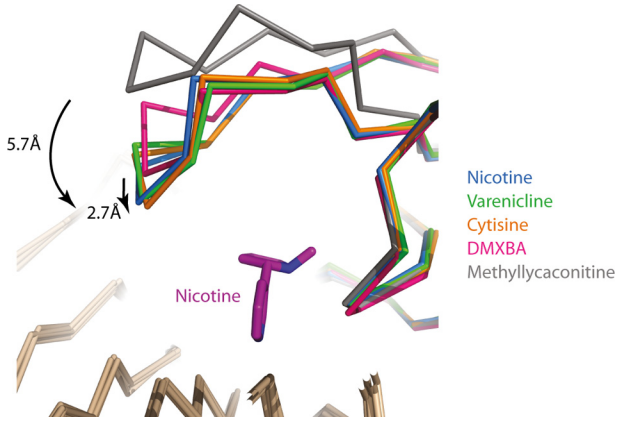

FIGURE 4. **Ribbon representation of LsAChBP in complex with nicotine (*blue*), cytisine (*orange*), varenicline (*green*), methyllycaconitine (*gray*, PDB code 2BYR) and DMXBA (*pink*, PDB code 2WNJ) superposed with respect to their principal face.** Nicotine is represented as *sticks* to indicate the orientation of a full agonist in the binding site. The tip of loop C is displaced outwards by 5.7 Å when AcAChBP is bound to the α7 nAChR antagonist methyllycaconitine and by 2.7 Å when AcAChBP is bound to partial agonist DMXBA when compared with the nicotine-bound state. No significant difference in the position of loop C is measured when AcAChBP is bound to nicotine, cytisine, or varenicline.

by a conserved tryptophan in nAChRs and that the AcAChBP Ser-165 resides in a region displaying low sequence similarity (Fig. 2*E*). The effect of such a modification to the ligand on the partial agonist nature of varenicline also remains to be investigated.

Correlating Binding Modes with Full or Partial Agonist Activity—In this study we included ligands acting either as a full agonist (nicotine) or as partial agonists (cytisine and varenicline) at the $\alpha4\beta2$ nAChR subtype. AChBP does not contain a transmembrane domain, but it has previously been shown that when coupled to the transmembrane domain of the 5HT3A receptor, it can trigger low frequency opening of the ion channel upon the application of acetylcholine (45). This suggests that AChBP comprises the required structural elements to connect ligand binding to channel opening.

The degree of loop C closure in AChBPs has been formerly correlated to the binding of agonists or antagonists (17, 18, 46, 47). Bulky antagonist binding to AChBP results in the outward movement of loop C, whereas small molecule agonist binding leads to the C loop closing in on the binding site. Recently, the structural characterization of AChBP in complex with DMXBA, a weak α7 nAChR partial agonist, suggested that partial agonism could result from multiple binding modes in the ligand binding site (48). These different binding poses reflect both typical agonist and antagonist binding modes and correlate with different degrees of loop C closure.

Interestingly, we could not detect any significant variation in the extent of the C loop closure over the binding site when comparing the co-crystal structure of LsAChBP in complex with a full $\alpha4\beta2$ nAChR agonist such as nicotine to those in complex with the partial agonists cytisine and varenicline (Fig. 4). Indeed, in our ligand-AcAChBP structures, the C loops are further closed upon the binding site when compared with the methyllycaconitine (antagonist)-bound structure (5.7 Å) or even to the DMXBA (α7 nAChR partial agonist)-bound structure (2.7 Å). Neither cytisine nor varenicline displayed variable binding modes in AcAChBP, with the ligands adopting the same orientation in all their respective binding sites.

The main difference we observed between the binding modes of nicotine to LsAChBP compared with cytisine or varenicline is that both partial agonists interact with the phenolic hydroxyl group of Tyr-91 (Fig. 2, *B*, *C*, and *E*). In AcAChBP Tyr-91 makes a hydrogen bond with the backbone carbonyl of Ser-144 through its hydroxyl group. This hydrogen bond is disrupted through the binding of lobeline to AcAChBP (supplemental Fig. S2). Lobeline, known to display a mixed agonist/antagonist mode of action toward nAChRs, is accommodated in the AcAChBP binding site through a reorientation of the Tyr-91 side chain, which makes hydrogen bonds to Tyr-53 and Ser-165 (17, 24). It is nevertheless unlikely that the interaction of a ligand with Tyr-91 would be sufficient to entail partial agonism. Indeed, epibatidine, which functions as a full agonist against the $\alpha4\beta2$ nAChRs, can also make a hydrogen bond to the Tyr-91 AcAChBP hydroxyl group via its bridge ring amine (17) (supplemental Fig. S2).

Recently, it has been shown that varenicline acts as a potent agonist against the human 5-hydroxytryptamine 3 receptor (5HT3AR), whereas its efficacy is limited at the mouse 5HT3AR (49). This difference in efficacy was rationalized in part by docking trials performed in homology-modeled ligand binding domains of the human and mouse receptors, which suggest that varenicline adopts different binding modes in these two proteins. Differences in binding modes are attributed to differences in the human and mouse 5HT3AR loops C, which in turn lead to differences in the orientation of conserved residue side chains. One such residue, displaying differences in orientation between the human and mouse, seems to be Glu-129, which lies on an equivalent loop to the one that harbors Tyr-91 in AcAChBP. Nevertheless, whereas both the AChBP and 5HT3AR ligand binding sites contain residues making up aromatic cages, the relative positions of aromatic residues vary and are likely to be reflected in the orientation adopted by varenicline in these two binding sites.

Our structural characterization of $\alpha4\beta2$ nAChR partial agonists in complex with AcAChBP suggest that whereas variability in the ligand binding modes is possibly one of the features that entails partial agonism to ligands, it is likely that this is not the only criterion for partial agonism. This study does not take into account the heteropentameric nature of the $\alpha4\beta2$ nAChR, which is likely to also be critical in the definition of partial and full agonist characteristics for ligands. Further work would be required, ideally on full receptors, to better understand the mechanisms underlying partial agonism.

Rationalizing Binding Affinity Differences of Nicotinic Ligands to $\alpha4\beta2$ and $\alpha7$ nAChR Subtypes—Cytisine, varenicline, and nicotine are all small (162–211 $gmol^{-1}$), high affinity binders for the $\alpha4\beta2$ nAChRs, but all display lower affinity for the $\alpha7$ subtype receptor (Table 2). From this initial observation, we went on to define which residues in the binding sites of these two receptor subtypes are responsible for such a large affinity difference in the binding of these molecules to these nAChRs. Our co-crystal structures with these ligands have confirmed their binding modes to AcAChBP, and together with a structure-based sequence alignment (Fig. 5) (50) have allowed us to

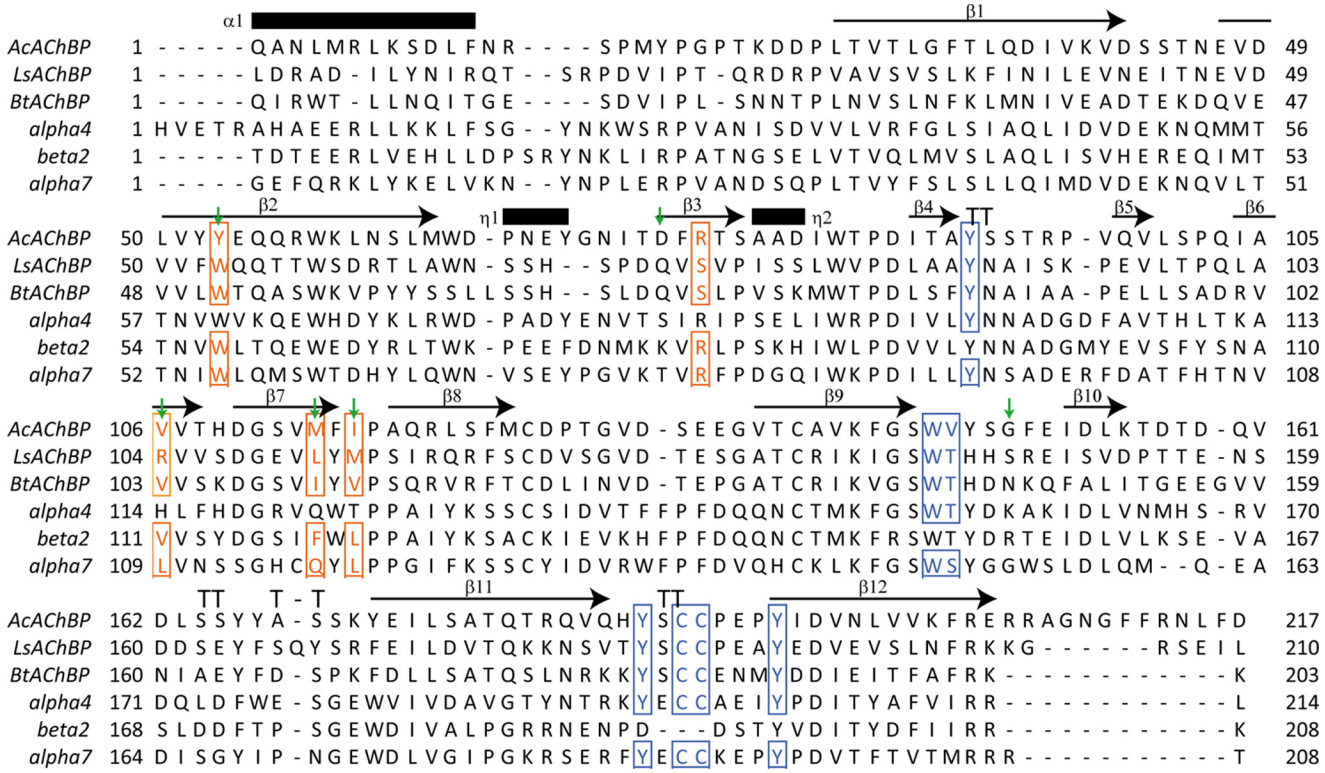

FIGURE 5. **Structure-based sequence alignment (50) of Ac-, Ls- ,and BtAChBPs with the α4, β2, and α7 nAChR subunits.** Ligand binding site residues involved in nicotine binding are *boxed*. Principal face residues are colored and boxed in *blue*, whereas complementary face ligand binding residues are colored and *boxed* in *orange*. Residues that were mutated to reflect α4β2 and α7 nAChRs are indicated by a *vertical green arrow*.

TABLE 3

K_D values obtained either from [^{3}H]cytisine saturation (S) radioligand binding or [^{3}H]cytisine homologous competition (HC) experiments are reported for different AcAChBP mutants

Binding curves for these proteins to cytisine are provided in supplemental Fig. S3 and S4.

Mutant	K_D	Method
	nM	
Wt	222 ± 35	HC
Y53W	5.5 ± 0.5	S
Y53W/I116L	38 ± 7	HC
G149K	40 ± 9	HC
Y53W/G149K	3.9 ± 0.3	S
Y53W/D75K	9 ± 1	S
Y53W/M114F	21 ± 6	HC
Y53W/I116L/G149K	10 ± 2	S
Y53W/I116L/D75K	100 ± 15	HC
Y53W/D75T	14 ± 2	HC
Y53W/I116L/D75T	193 ± 17	HC
Y53W/I116L/M114Q	200 ± 30	HC
Y53W/I116L/V106L	56 ± 6	HC
Y53W/I116L/D75T/M114Q	186 ± 11	HC

map out residues likely to be involved in binding these molecules in α4β2 or in α7 nAChR subtypes. We implemented both single and combined mutations into AcAChBP so that the binding site of the resulting protein would reflect either that of the α4β2 or of the α7 receptor subtype. The mutations (Fig. 5) address residues directly in contact with the ligands in the binding site and residues previously reported to influence agonist binding to nAChRs such as G149K (AcAChBP numbering) (51). The different mutants generated were subjected to [^{3}H]cytisine saturation or homologous competition binding assays.

Overall, AcAChBP mutants engineered to reflect the α7 nAChR binding site showed a lower affinity for cytisine when compared with α4β2 like mutants (Table 3). Indeed, combining α7 like mutations D75T or M114Q into Y53W- or Y53W/I116L-AcAChBPs resulted in affinity loss for cytisine when compared with their α4β2 counterparts (Fig. 6, *A* and *B*), whereas epibatidine binding levels were not significantly altered for the same mutants. This result demonstrates that complementary face binding site residues are critical for subtype-selective ligand binding in nAChRs.

Among the mutants we generated to reflect the α4β2 binding site, the Y53W/G149K AcAChBP mutant displayed the largest gain in affinity toward cytisine compared with wt-AcAChBP (57-fold) (Fig. 6, *A* and *B*). Previous reports show that mutating the α7 nAChR Gly-152 to a lysine as present in α4β2 increases agonist binding affinity (102-fold toward nicotine) and increases acetylcholine potency (7-fold) (51). Similarly, mutating the α1 nAChR Gly-153 to a lysine also increased nicotine affinity for the receptor, most likely by making the binding site more accessible for agonist binding through the formation of a hydrogen bond between loops B and C (52). Such a hydrogen bond is already present in AcAChBP despite the presence of a glycine at position 149 (Fig. 5), and the G149K mutation in AcAChBP does not entail a drastic affinity improvement (1.7-fold) over wt-AcAChBP. Our results indicate that mutating the AcAChBP tyrosine 53 into a tryptophan significantly enhances cytisine binding affinity, with a 40-fold decrease in the K_D (Fig. 6*A*), in line with previous results for other nicotinic agonists (17). We could not identify other mutations that result in improved affinity toward cytisine compared with the Y53W/G149K mutant. The M114F mutation results in a 4-fold decreased affinity for cytisine compared with Y53W-

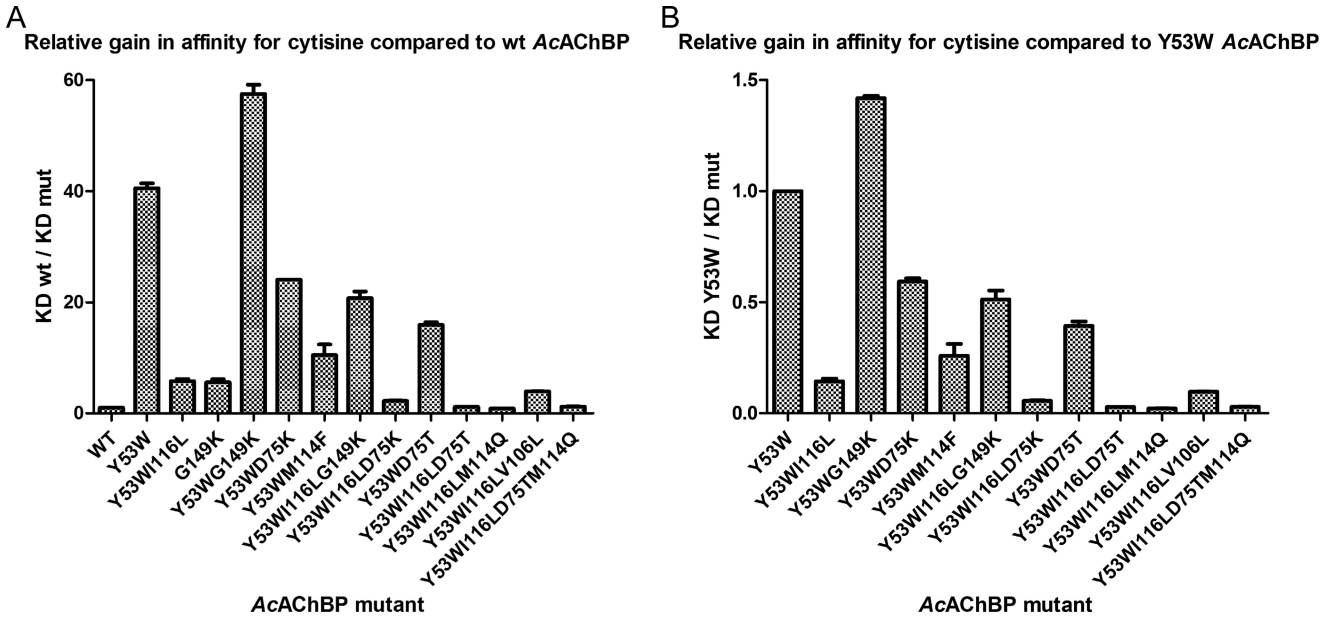

FIGURE 6. ***Bar charts* representing the improvement in binding affinity of selected mutants with respect to wild type AcAChBP (*A*) or to AcAChBP incorporating the Y53W mutation (*B*).** Improvement in affinity was measured as the ratio of affinities (K_D) of either wild type (*A*) or Y53W (*B*) AcAChBPs to those of other AcAChBP mutants. Errors were propagated from initial radioligand binding measurements (Table 2).

AcAChBP, probably because the side chain of the phenylalanine is forced into an unusual rotamer orientation to avoid clashes with residues Arg-57, Val-106, or Ile-116. A 7-fold decrease in affinity was also observed when comparing the Y53W/I116L mutant to Y53W, suggesting that the leucine side chain also has to adopt an unusual rotamer orientation to prevent clashes with Tyr-53, Gln-55, or Trp-145. Switching Asp-75 to a lysine in the Y53W/D75K mutant results in a 2-fold decrease in affinity compared with Y53W AcAChBP. Thus modifications in the first shell of binding site residues are not sufficient to mimic the high affinity of the $\alpha4\beta2$ nAChRs for cytisine. This suggests that residues beyond the first shell of binding are critical for the high affinity interaction, as was previously suggested for other receptor subtypes (52).

A similar mutational approach based on structural information has been previously used to understand the difference in nicotine binding affinity between *B. truncatus* AChBP (BtAChBP) (K_D = 8 nM) and LsAChBP (K_D = 45 nM) (15). In this study three amino acid substitutions within the first shell of ligand binding were sufficient to improve the affinity of LsAChBP to the level of BtAChBP. The comparison between Ls- and BtAChBP structures suggested that the direct interactions with the side chains of these amino acids were critical in defining nicotine affinity (15). In this study we have extended this approach to investigate differences in affinity in the binding of cytisine to the $\alpha7$ and $\alpha4\beta2$ nAChRs. However, contrary to the previous study (15), mutating AcAChBP binding site residues to their $\alpha4\beta2$ counterparts did not drastically improve cytisine binding affinities. This result strongly suggests that the orientation of binding site residue side chains is influenced not only by residues at the protomer-protomer interface but also by residues located outside of the ligand binding site, such as Gly-152. We believe that these residues modulate the geometry of the ligand binding site and hence the orientation of binding site residue side chains through long range interactions, entailing affinity differences during ligand binding.

We have used AChBP as a template to investigate the binding modes of three different molecules, nicotine, cytisine, and varenicline, targeted toward the $\alpha4\beta2$ nAChR in smoking cessation therapies. The ITC data we recorded provide a rationale for differences in binding of these three ligands to AcAChBP, and our structural data provide the binding orientations of these molecules, allowing us to define binding site residues interacting with these ligands. Importantly, we find that all three ligands have similar binding poses. The detailed structures provide insight in the effect of possible chemical changes in these compounds.

Our mutational analysis of the AcAChBP binding site shows that complementary binding site residues are critical but not sufficient to entail subtype selective ligand binding to nAChRs. The decrease in affinity observed for $\alpha4\beta2$-like mutants for cytisine suggests that complementary face residues from the binding site are probably not properly oriented for high affinity ligand binding. The orientation of residues in this primary shell of binding residues is very likely to be plastic in nature and can be influenced by longer range interactions extending farther from the ligand binding site.

Acknowledgments—We thank the staff from SLS PXI and ESRF beamlines ID23-EH2 and ID14-EH4 for assistance during data collection and Robbie Joosten and Anastassis Perrakis for useful discussions during the refinement and data validation steps. We also thank Mark Hilge (Radboud University, Nijmegen) for use of and assistance with the ITC200 system.

REFERENCES

1. Rucktooa, P., Smit, A. B., and Sixma, T. K. (2009) Insight in nAChR subtype selectivity from AChBP crystal structures. *Biochem. Pharmacol.* **78,**

777–787
2. Corringer, P. J., Le Novère, N., and Changeux, J. P. (2000) Nicotinic receptors at the amino acid level. *Annu. Rev. Pharmacol. Toxicol.* **40,** 431–458
3. Karlin, A. (2002) Emerging structure of the nicotinic acetylcholine receptors. *Nat. Rev. Neurosci.* **3,** 102–114
4. Sine, S. M., and Engel, A. G. (2006) Recent advances in Cys-loop receptor structure and function. *Nature* **440,** 448–455
5. Unwin, N. (1993) Nicotinic acetylcholine receptor at 9 Angstrom resolution. *J. Mol. Biol.* **229,** 1101–1124
6. Unwin, N. (2005) Refined structure of the nicotinic acetylcholine receptor at 4 Å resolution. *J. Mol. Biol.* **346,** 967–989
7. Brejc, K., van Dijk, W. J., Klaassen, R. V., Schuurmans, M., van Der Oost, J., Smit, A. B., and Sixma, T. K. (2001) Crystal structure of an ACh-binding protein reveals the ligand binding domain of nicotinic receptors. *Nature* **411,** 269–276
8. Smit, A. B., Syed, N. I., Schaap, D., van Minnen, J., Klumperman, J., Kits, K. S., Lodder, H., van der Schors, R. C., van Elk, R., Sorgedrager, B., Brejc, K., Sixma, T. K., and Geraerts, W. P. (2001) A glia-derived acetylcholine-binding protein that modulates synaptic transmission. *Nature* **411,** 261–268
9. Dellisanti, C. D., Yao, Y., Stroud, J. C., Wang, Z. Z., and Chen, L. (2007) Crystal structure of the extracellular domain of nAChR α1 bound to α-bungarotoxin at 1.94 Å resolution. *Nat. Neurosci.* **10,** 953–962
10. Bocquet, N., Nury, H., Baaden, M., Le Poupon, C., Changeux, J. P., Delarue, M., and Corringer, P. J. (2009) X-ray structure of a pentameric ligand-gated ion channel in an apparently open conformation. *Nature* **457,** 111–114
11. Hilf, R. J., and Dutzler, R. (2008) X-ray structure of a prokaryotic pentameric ligand-gated ion channel. *Nature* **452,** 375–379
12. Hilf, R. J., and Dutzler, R. (2009) Structure of a potentially open state of a proton-activated pentameric ligand-gated ion channel. *Nature* **457,** 115–118
13. Hibbs, R. E., and Gouaux, E. (2011) Principles of activation and permeation in an anion-selective Cys-loop receptor. *Nature* **474,** 54–60
14. Celie, P. H., van Rossum-Fikkert, S. E., van Dijk, W. J., Brejc, K., Smit, A. B., and Sixma, T. K. (2004) Nicotine and carbamylcholine binding to nicotinic acetylcholine receptors as studied in AChBP crystal structures. *Neuron* **41,** 907–914
15. Celie, P. H., Klaassen, R. V., van Rossum-Fikkert, S. E., van Elk, R., van Nierop, P., Smit, A. B., and Sixma, T. K. (2005) Crystal structure of acetylcholine-binding protein from *Bulinus truncatus* reveals the conserved structural scaffold and sites of variation in nicotinic acetylcholine receptors. *J. Biol. Chem.* **280,** 26457–26466
16. Sine, S. M., Kreienkamp, H. J., Bren, N., Maeda, R., and Taylor, P. (1995) Molecular dissection of subunit interfaces in the acetylcholine receptor. Identification of determinants of α-conotoxin M1 selectivity. *Neuron* **15,** 205–211
17. Hansen, S. B., Sulzenbacher, G., Huxford, T., Marchot, P., Taylor, P., and Bourne, Y. (2005) Structures of *Aplysia* AChBP complexes with nicotinic agonists and antagonists reveal distinctive binding interfaces and conformations. *EMBO J.* **24,** 3635–3646
18. Ulens, C., Hogg, R. C., Celie, P. H., Bertrand, D., Tsetlin, V., Smit, A. B., and Sixma, T. K. (2006) Structural determinants of selective α-conotoxin binding to a nicotinic acetylcholine receptor homolog AChBP. *Proc. Natl. Acad. Sci. U.S.A.* **103,** 3615–3620
19. Dwoskin, L. P., Smith, A. M., Wooters, T. E., Zhang, Z., Crooks, P. A., and Bardo, M. T. (2009) Nicotinic receptor-based therapeutics and candidates for smoking cessation. *Biochem. Pharmacol.* **78,** 732–743
20. Benowitz, N. L. (2010) Nicotine addiction. *N. Engl. J. Med.* **362,** 2295–2303
21. Daly, J. W. (2005) Nicotinic agonists, antagonists, and modulators from natural sources. *Cell. Mol. Neurobiol.* **25,** 513–552
22. Lancaster, T., Stead, L., and Cahill, K. (2008) An update on therapeutics for tobacco dependence. *Expert Opin. Pharmacother.* **9,** 15–22
23. Coe, J. W., Brooks, P. R., Vetelino, M. G., Wirtz, M. C., Arnold, E. P., Huang, J., Sands, S. B., Davis, T. I., Lebel, L. A., Fox, C. B., Shrikhande, A., Heym, J. H., Schaeffer, E., Rollema, H., Lu, Y., Mansbach, R. S., Chambers, L. K., Rovetti, C. C., Schulz, D. W., Tingley, F. D., 3rd, and O'Neill, B. T. (2005) Varenicline. An $\alpha4\beta2$ nicotinic receptor partial agonist for smoking cessation. *J. Med. Chem.* **48,** 3474–3477
24. Edink, E., Rucktooa, P., Retra, K., Akdemir, A., Nahar, T., Zuiderveld, O., van Elk, R., Janssen, E., van Nierop, P., van Muijlwijk-Koezen, J., Smit, A. B., Sixma, T. K., Leurs, R., and de Esch, I. J. (2011) Fragment growing induces conformational changes in acetylcholine-binding protein. A structural and thermodynamic analysis. *J. Am. Chem. Soc.* **133,** 5363–5371
25. Kabsch, W. (2010) Integration, scaling, space-group assignment, and post-refinement. *Acta Crystallogr. D Biol. Crystallogr.* **66,** 133–144
26. Kabsch, W. (2010) XDS. *Acta Crystallogr. D Biol. Crystallogr.* **66,** 125–132
27. Evans, P. (2006) Scaling and assessment of data quality. *Acta Crystallogr. D Biol. Crystallogr.* **62,** 72–82
28. McCoy, A. J., Grosse-Kunstleve, R. W., Adams, P. D., Winn, M. D., Storoni, L. C., and Read, R. J. (2007) Phaser crystallographic software. *J. Appl. Crystallogr.* **40,** 658–674
29. Celie, P. H., Kasheverov, I. E., Mordvintsev, D. Y., Hogg, R. C., van Nierop, P., van Elk, R., van Rossum-Fikkert, S. E., Zhmak, M. N., Bertrand, D., Tsetlin, V., Sixma, T. K., and Smit, A. B. (2005) Crystal structure of nicotinic acetylcholine receptor homolog AChBP in complex with an α-conotoxin PnIA variant. *Nat. Struct. Mol. Biol.* **12,** 582–588
30. Murshudov, G. N., Vagin, A. A., and Dodson, E. J. (1997) Refinement of macromolecular structures by the maximum likelihood method. *Acta Crystallogr. D Biol. Crystallogr.* **53,** 240–255
31. Bricogne, G., B. E., Brandl, M., Flensburg, C., Keller, P., Paciorek, W., and Roversi, P, S. A., Smart, O. S., Vonrhein, C., Womack, T. O. (2011) BUSTER, 2.8.0. Ed., Global Phasing Ltd., Cambridge, United Kingdom
32. Joosten, R. P., Joosten, K., Cohen, S. X., Vriend, G., and Perrakis, A. (2011) Automatic rebuilding and optimization of crystallographic structures in the Protein Data Bank. *Bioinformatics* **27,** 3392–3398
33. Emsley, P., Lohkamp, B., Scott, W. G., and Cowtan, K. (2010) Features and development of Coot. *Acta Crystallogr. D Biol. Crystallogr.* **66,** 486–501
34. Chen, V. B., Arendall, W. B., 3rd, Headd, J. J., Keedy, D. A., Immormino, R. M., Kapral, G. J., Murray, L. W., Richardson, J. S., and Richardson, D. C. (2010) Cloning, recombinant production, crystallization, and preliminary X-ray diffraction analysis of SDF2-like protein from *Arabidopsis thaliana*. *Acta Crystallogr. D Biol. Crystallogr.* **66,** 12–21
35. Eaton, J. B., Peng, J. H., Schroeder, K. M., George, A. A., Fryer, J. D., Krishnan, C., Buhlman, L., Kuo, Y. P., Steinlein, O., and Lukas, R. J. (2003) Characterization of human $\alpha4\beta2$-nicotinic acetylcholine receptors stably and heterologously expressed in native nicotinic receptor-null SH-EP1 human epithelial cells. *Mol. Pharmacol.* **64,** 1283–1294
36. Chellappan, S. K., Xiao, Y., Tueckmantel, W., Kellar, K. J., and Kozikowski, A. P. (2006) Synthesis and pharmacological evaluation of novel 9- and 10-substituted cytisine derivatives. Nicotinic ligands of enhanced subtype selectivity. *J. Med. Chem.* **49,** 2673–2676
37. Kozikowski, A. P., Chellappan, S. K., Xiao, Y., Bajjuri, K. M., Yuan, H., Kellar, K. J., and Petukhov, P. A. (2007) Chemical medicine. Novel 10-substituted cytisine derivatives with increased selectivity for $\alpha4\beta2$ nicotinic acetylcholine receptors. *ChemMedChem* **2,** 1157–1161
38. Imming, P., Klaperski, P., Stubbs, M. T., Seitz, G., and Gündisch, D. (2001) Syntheses and evaluation of halogenated cytisine derivatives and of bioisosteric thiocytisine as potent and selective nAChR ligands. *Eur. J. Med. Chem.* **36,** 375–388
39. Slater, Y. E., Houlihan, L. M., Maskell, P. D., Exley, R., Bermúdez, I., Lukas, R. J., Valdivia, A. C., and Cassels, B. K. (2003) Halogenated cytisine derivatives as agonists at human neuronal nicotinic acetylcholine receptor subtypes. *Neuropharmacology* **44,** 503–515
40. Carbonnelle, E., Sparatore, F., Canu-Boido, C., Salvagno, C., Baldani-Guerra, B., Terstappen, G., Zwart, R., Vijverberg, H., Clementi, F., and Gotti, C. (2003) Nitrogen substitution modifies the activity of cytisine on neuronal nicotinic receptor subtypes. *Eur. J. Pharmacol.* **471,** 85–96
41. Tasso, B., Canu Boido, C., Terranova, E., Gotti, C., Riganti, L., Clementi, F., Artali, R., Bombieri, G., Meneghetti, F., and Sparatore, F. (2009) Synthesis, binding, and modeling studies of new cytisine derivatives as ligands for neuronal nicotinic acetylcholine receptor subtypes. *J. Med. Chem.* **52,** 4345–4357
42. Abin-Carriquiry, J. A., Zunini, M. P., Cassels, B. K., Wonnacott, S., and

Dajas, F. (2010) In silico characterization of cytisinoids docked into an acetylcholine binding protein. *Bioorg. Med. Chem. Lett.* **20,** 3683–3687
43. Huang, X., Zheng, F., Chen, X., Crooks, P. A., Dwoskin, L. P., and Zhan, C. G. (2006) Modeling subtype-selective agonists binding with $\alpha4\beta2$ and $\alpha7$ nicotinic acetylcholine receptors. Effects of local binding and long range electrostatic interactions. *J. Med. Chem.* **49,** 7661–7674
44. Krissinel, E., and Henrick, K. (2007) Inference of macromolecular assemblies from crystalline state. *J. Mol. Biol.* **372,** 774–797
45. Bouzat, C., Gumilar, F., Spitzmaul, G., Wang, H. L., Rayes, D., Hansen, S. B., Taylor, P., and Sine, S. M. (2004) Coupling of agonist binding to channel gating in an ACh-binding protein linked to an ion channel. *Nature* **430,** 896–900
46. Bourne, Y., Talley, T. T., Hansen, S. B., Taylor, P., and Marchot, P. (2005) Crystal structure of a Cbtx-AChBP complex reveals essential interactions between snake α-neurotoxins and nicotinic receptors. *EMBO J.* **24,** 1512–1522
47. Shi, J., Koeppe, J. R., Komives, E. A., and Taylor, P. (2006) Ligand-induced conformational changes in the acetylcholine-binding protein analyzed by hydrogen-deuterium exchange mass spectrometry. *J. Biol. Chem.* **281,** 12170–12177
48. Hibbs, R. E., Sulzenbacher, G., Shi, J., Talley, T. T., Conrod, S., Kem, W. R., Taylor, P., Marchot, P., and Bourne, Y. (2009) Structural determinants for interaction of partial agonists with acetylcholine-binding protein and neuronal $\alpha7$ nicotinic acetylcholine receptor. *EMBO J.* **28,** 3040–3051
49. Lummis, S. C., Thompson, A. J., Bencherif, M., and Lester, H. A. (2011) Varenicline is a potent agonist of the human 5-hydroxytryptamine 3 receptor. *J. Pharmacol. Exp. Ther.* **339,** 125–131
50. Notredame, C., Higgins, D. G., and Heringa, J. (2000) T-Coffee. A novel method for fast and accurate multiple sequence alignment. *J. Mol. Biol.* **302,** 205–217
51. Grutter, T., Prado de Carvalho, L., Le Novère, N., Corringer, P. J., Edelstein, S., and Changeux, J. P. (2003) An H-bond between two residues from different loops of the acetylcholine binding site contributes to the activation mechanism of nicotinic receptors. *EMBO J.* **22,** 1990–2003
52. Xiu, X., Puskar, N. L., Shanata, J. A., Lester, H. A., and Dougherty, D. A. (2009) Nicotine binding to brain receptors requires a strong cation-π interaction. *Nature* **458,** 534–537
53. Krissinel, E., and Henrick, K. (2004) Secondary-structure matching (SSM), a new tool for fast protein structure alignment in three dimensions. *Acta Crystallogr. D Biol. Crystallogr.* **60,** 2256–2268